OPEN ACCESS

Scholars International Journal of Chemistry and Material Sciences

Abbreviated Key Title: Sch Int J Chem Mater Sci
ISSN 2616-8669 (Print) |ISSN 2617-6556 (Online)
Scholars Middle East Publishers, Dubai, United Arab Emirates
Journal homepage: http://saudijournals.com

Original Research Article

Production of MgO/ZnO Nanocomposite for the Removal of Selected Toxic Metals from Tannery Wastewater

Aisha Abdulkadir[1]*, Monday Musah[1], Ibrahim Isah Lakan[1], John Tsado Mathew[1]

[1]Department of Chemistry, Ibrahim Badamasi Babangida University, Lapai, Niger State, Nigeria

DOI: https://doi.org/10.36348/sijcms.2025.v08i05.008 | **Received:** 26.08.2025 | **Accepted:** 15.10.2025 | **Published:** 25.10.2025

***Corresponding author:** Aisha Abdulkadir
Department of Chemistry, Ibrahim Badamasi Babangida University, Lapai, Niger State, Nigeria

Abstract

Leather industry is a significant source of industrial wastewater pollution with effluent that is high in toxic metals like chromium (Cr), cadmium (Cd), lead (Pb), and iron (Fe). The contaminants are very dangerous to the environment and human health because of their toxicity, persistence and their potential to accumulate bio-accumulate. The research problem under study involves the creation of a magnesium oxide/zinc oxide (MgO/ZnO) nanocomposite that has a high selectivity in the removal of specific toxic metals in the tannery wastewater. A co-precipitation technique was used to produce the nanocomposite, which was then heated at 450ºC to produce a crystalline material with improved surface properties. The successful formation of the nanocomposite and high surface reactivity of the nanocomposite were confirmed using characterization methods such as X-ray diffraction (XRD), Fourier-transform infrared spectroscopy (FTIR), scanning electron microscopy (SEM), and Brunauer Bfer Emmett Teller surface area analysis. The experiments of batch adsorption were performed to determine the influence of the pH, contact time, dosage of adsorbent, and the initial concentration of metal on the efficiency of removal. Findings indicated that the MgO/ZnO nanocomposite had a high adsorption capacity, which reached high levels of toxic metals reduction under the conditions of optimal parameters. The data of adsorption were well-fitted with Langmuir and Freundlich isotherm models of adsorption, which showed monolayer and heterogeneous adsorption. These results indicate that MgO/ZnO nanocomposites could be used as an economical and sustainable substitute of the treatment of tannery wastewater, and has a possibility of large scale uses in industrial wastewater treatment.

Keywords: Metals, Nanocomposite, Tannery, Toxic, Treatment, Wastewater.

INTRODUCTION

The development of the leather industry has been very beneficial to the world economy as it has offered job opportunities and made a variety of leather goods. Nevertheless, such an industrial process is also a primary contributor to water pollution, mostly via release of untreated or partially treated tannery wastewater into natural water sources. Tannery effluent bears dark colour, high organic load and toxic heavy metal chemicals, which include chromium (Cr), lead (Pb), cadmium (Cd) and iron (Fe), which are consumed in the process of tanning and finishing. These toxic metals are of special interest because of their persistence, their ability to bioaccumulate and their gross health effects on humans and aquatic organisms. Cases of neurological disorders, kidney damage, carcinogenicity and enzymatic system disruption have been associated with prolonged exposure to heavy metals (Milanković *et al.* 2024). These traditional treatment methods currently used in most developing nations such as chemical precipitation, coagulation-flocculation and biological treatment method are usually inadequate in full removal of toxic metals, resulting in soil and ground water pollution. This escalating difficulty exemplifies the critical concern of cost effective and efficacy treatment technologies that can deal with the intricacy of the tannery wastewater (Mathew *et al.* 2024a).

Nanotechnology has provided a potential solution in the area of wastewater treatment by providing high-quality physicochemical materials that can be used to improve adsorption, photocatalysis, and the efficacy of contaminant elimination. Magnesium oxide (MgO) and zinc oxide (ZnO) are the metal oxide nanomaterials that have attracted a lot of attention because they possess high surface area, tunable surface chemistry, stability, and high adsorption capacity of heavy metal ions (Sazid, and Supto, 2025). MgO nanoparticles boast of excellent basicity, high reactivity as well as a high affinity with acidic contaminants that makes them very useful in binding and immobilizing toxic metal ions. Likewise, ZnO nanoparticles have special photocatalytic and antibacterial features that aid in the breakdown of the organic pollutants and disinfection of wastewater (Rezania *et al.,* 2024). Through this combination of MgO and ZnO into a nanocomposite, it can be utilized to take advantage of their interactions leading to higher adsorption of pollutants, increased stability, and higher removal of a broad spectrum of pollutants than its constituent components. Also, nanocomposites can be designed such that they contain hierarchical porosity and functional groups that have selectivity to toxic metal ions, which provide a sustainable answer to industrial wastewater treatment (Ibrahim *et al.,* 2025).

MgO/ZnO nanocomposites as a prospective treatment system in tannery wastewater treatment are thus an excellent and timely study. Additionally, the use of nanocomposite-based treatment can be combined with the conventional systems of treatment that are already in place to enhance their performance without introducing serious operational cost impacts. The purpose of the study is to synthesize and characterize MgO/ZnO nanocomposites through environmentally friendly and cost-effective processes, determine the effectiveness of the nanocomposites in the removal of the specific toxic metals present in tannery wastewater, and determine optimal parameters of pH, contact time, and dosage of the adsorbent (Ameen, 2023). The results of this study may help in the design of scalable treatment technologies in the leather business, reduce the environmental and health risks linked with tannery effluents, and promote sustainable business conduct in accordance with the global environmental protection objectives.

MATERIALS AND METHODS

This study was designed to synthesize, characterize, and evaluate the performance of MgO/ZnO nanocomposites for the removal of selected toxic metals from tannery wastewater. The methodology involved four key stages: (i) collection and pre-treatment of tannery wastewater, (ii) synthesis of the MgO/ZnO nanocomposite, (iii) characterization of the synthesized material, and (iv) batch adsorption experiments to evaluate its performance under controlled conditions. All experimental procedures were conducted following standard guidelines for wastewater treatment research and under safe laboratory practices (Mathew *et al.* 2023a; Muhammad *et al.* 2024).

Collection and Pre-Treatment of Tannery Wastewater

Raw tannery wastewater was collected from a leather-processing facility, preferably during peak production hours to ensure representativeness of contaminant levels. The wastewater samples were collected in pre-cleaned polyethylene containers, transported to the laboratory under cold conditions, and stored at 4 °C prior to analysis and use. Preliminary characterization of the wastewater was conducted to determine physicochemical parameters including pH, temperature. Concentrations of heavy metals such as chromium (Cr), cadmium (Cd), lead (Pb) and Iron (Fe) were measured using atomic absorption spectrophotometry (AAS). To remove suspended solids and other debris that could interfere with adsorption experiments, the wastewater was first filtered through Whatman No. 1 filter paper and then centrifuged at 3000 rpm for 15 minutes. The supernatant was used for all subsequent batch adsorption studies (Mathew *et al.* 2024c; Musah, et al. 2025).

Synthesis of MgO/ZnO Nanocomposite

The MgO/ZnO nanocomposite was synthesized using a co-precipitation method due to its simplicity, scalability, and ability to produce homogeneous nanomaterials with high purity. Analytical-grade magnesium nitrate hexahydrate [$Mg(NO_3)_2 \cdot 6H_2O$] and zinc nitrate hexahydrate [$Zn(NO_3)_2 \cdot 6H_2O$] were used as precursors, while sodium hydroxide (NaOH) served as the precipitating agent. Briefly, stoichiometric amounts of magnesium and zinc nitrates were dissolved in deionized water under constant stirring to form a clear solution. The mixed solution was then heated to 60–70 °C and NaOH solution (1 M) was added dropwise under vigorous stirring until the pH reached 10–11, leading to the formation of a white precipitate. The precipitate was aged for 24 hours to promote crystal growth and then separated by centrifugation. The resulting solid was washed several times with deionized water and ethanol to remove residual nitrates and impurities. The washed product was dried in a hot air oven at 80 °C for 12 hours, followed by calcination in a muffle furnace at 450 °C for 3 hours to obtain the MgO/ZnO nanocomposite in crystalline form. The calcined product was ground into a fine powder and stored in airtight containers for further characterization and use (Musa *et al.* 2024; Mathew *et al.* 2024b).

Characterization of Synthesized Nanocomposite

The physicochemical and structural properties of the synthesized MgO/ZnO nanocomposite were analyzed using standard characterization techniques. The crystal structure was determined by X-ray diffraction (XRD), and the diffraction patterns were compared with standard Joint Committee on Powder Diffraction Standards (JCPDS) data to confirm phase composition. The surface morphology and particle size distribution were examined using scanning electron microscopy (SEM) while energy-dispersive X-ray spectroscopy (EDS) was employed to confirm elemental composition. Fourier-transform infrared spectroscopy (FTIR) was performed to identify surface functional groups and confirm the presence of metal–oxygen bonds. Additionally, the Brunauer–Emmett–Teller (BET) method was used to determine the specific surface area, pore volume, and pore size distribution of the nanocomposite, which are critical for adsorption performance (Idris *et al.* 2024; Mathew *et al.* 2025).

Batch Adsorption Experiments

The adsorption performance of the MgO/ZnO nanocomposite was evaluated through batch experiments under varying experimental conditions. Known quantities of the nanocomposite were added to 100 cm^3 of pre-treated tannery wastewater in 250 cm^3conical flasks. The flasks were placed on an orbital shaker and agitated at 150 rpm for a fixed contact time. The effect of operational parameters such as pH (3–10), adsorbent dosage (0.1–2.0 g/100 cm^3), contact time (10–180 minutes), and initial metal ion concentration (10–100 mg/L) on adsorption efficiency was systematically investigated. After treatment, the samples were filtered, and residual metal concentrations were determined by AAS. The percentage removal of metal ions was calculated using the equation:

$$\text{Removal Efficiency (\%)} = \frac{C_0 - C_e}{C_0} \times 100$$

where $C_0$is the initial metal concentration and $C_e$is the equilibrium concentration after treatment.

Kinetic Studies

Adsorption isotherms were 252modelled using Langmuir and Freundlich equations to understand the adsorption mechanism and surface heterogeneity of the nanocomposite. Kinetic studies were performed by fitting experimental data to pseudo-first-order and pseudo-second-order models to evaluate the rate-controlling steps (Mathew *et al.* 2023b).

RESULTS AND DISCUSSION

From Table 1, Mg/ZnO nanocomposites reveals essential details about the morphology and structural properties of the nanoparticles. At a magnification of 1000x, the particles exhibit a relatively uniform distribution, with some degree of aggregation likely due to the inherent high surface energy of nanoparticles, which can lead to agglomeration (Kiran *et al.,* 2022). The 1269 µm field of view captures a wide area, providing valuable insight into the homogeneity of the composite structure. The accelerating voltage of 15 kV is optimal for achieving clear images of non-conductive materials, ensuring effective contrast for surface feature identification (Cortés *et al.,* 2022). The working distance of 8.770 mm supports high-resolution imaging, minimizing electron scattering effects, which is crucial for accurately capturing the fine details of the nanoparticles (Quintard *et al.,* 2025). Previous studies have shown that combining MgO with ZnO in nanocomposites often results in improved dispersion and stability, as the two oxides work synergistically to reduce aggregation and enhance properties like photocatalytic activity and antimicrobial effectiveness (Mtavangu *et al.,* 2022).

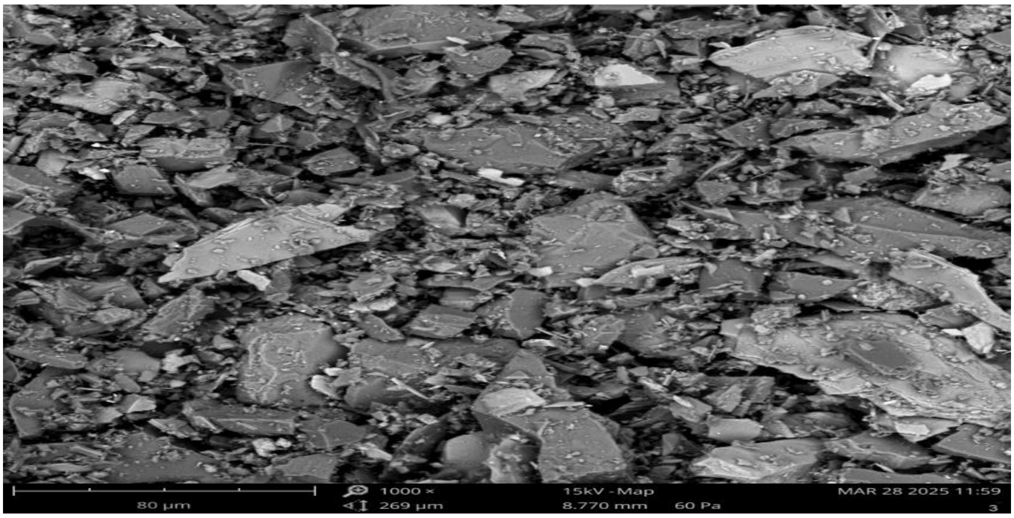

Figure 1: SEM Image of MgO/ZnO

The XRD analysis of Mg/ZnO nanocomposites (Fig. 2) displayed well-defined and sharp diffraction peaks, indicating a high degree of crystallinity. Major peaks were observed at 2θ values around 28°, 31°, 36°, and 47°, which correspond to the hexagonal wurtzite structure of Zincite (ZnO), confirming its presence as the primary phase. Additional peaks matched reference patterns for Periclase (MgO), Quartz (SiO_2), and Vesuvianite (a complex silicate), suggesting that the sample may contain minor impurity phases or unreacted precursors. The intensity count reaching up to 4000 cps indicates a highly crystalline structure, which enhances the functional properties of the composite (Alharbi *et al.,* 2023). These findings are in line with previous studies, which reported that Mg/ZnO nanocomposites show improved thermal stability, catalytic activity, and microbial resistance due to enhanced structural synergy and surface reactivity (Lallo da Silva *et al.,* 2019). Thus, the crystallinity and phase composition confirmed by the XRD analysis suggests the nanocomposite is suitable for multifunctional applications.

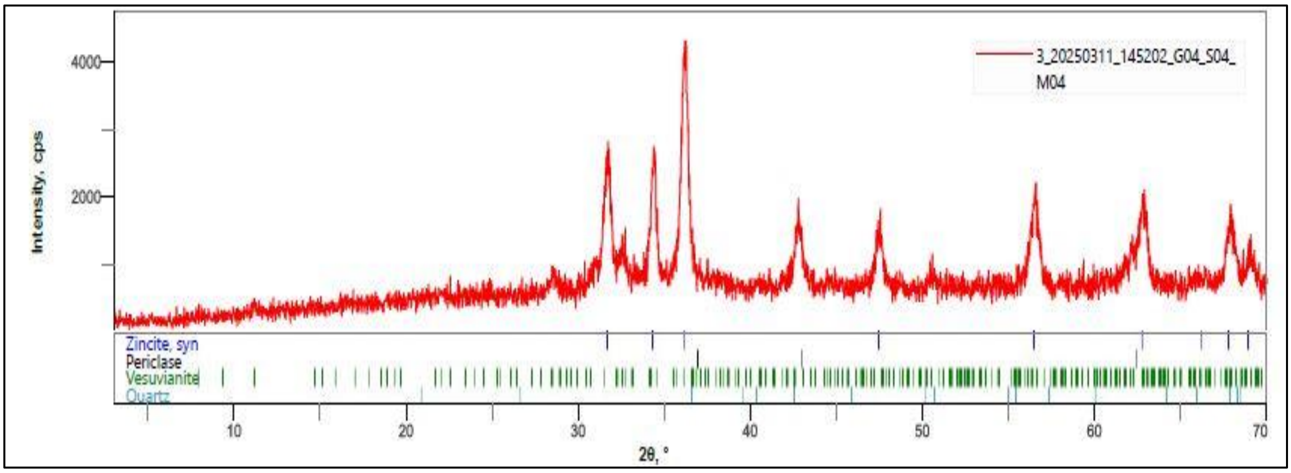

Figure 2: XRD Image of MgO/ZnO

The FTIR analysis of the Mg/ZnO nanocomposites (Fig. 3) reveals several significant peaks that confirm the formation of metal oxide nanostructures and the presence of functional groups from the synthesis process. A broad and moderate transmittance band at 3265.1 cm^{-1} is attributed to O–H stretching vibrations of hydroxyl groups or adsorbed moisture on the nanocomposite surface. This is a typical feature observed in metal oxide nanoparticles due to their high surface area and tendency to retain water molecules (Almoneef *et al.,* 2024). The peak observed at 1636.3 cm^{-1} corresponds to H–O–H bending vibrations of molecular water. The most prominent absorption bands appeared around 1032.5 cm^{-1} and 1080.9 cm^{-1}, which can be assigned to the metal–oxygen (M–O) stretching vibrations, particularly Zn–O and Mg–O bonds, confirming the formation of the Mg/ZnO composite structure. The transmittance data also show a relatively high intensity in this region, indicating strong and well-formed bonds between metal and oxygen atoms (Zhang *et al.,* 2024). These findings are consistent with recent literature, where similar bands were observed in Mg/ZnO systems synthesized via sol-gel or hydrothermal methods. Such FTIR results also suggest that the composite may have enhanced surface reactivity and antimicrobial properties due to hydroxyl and metal oxide group interactions (Redjili *et al.,* 2025).

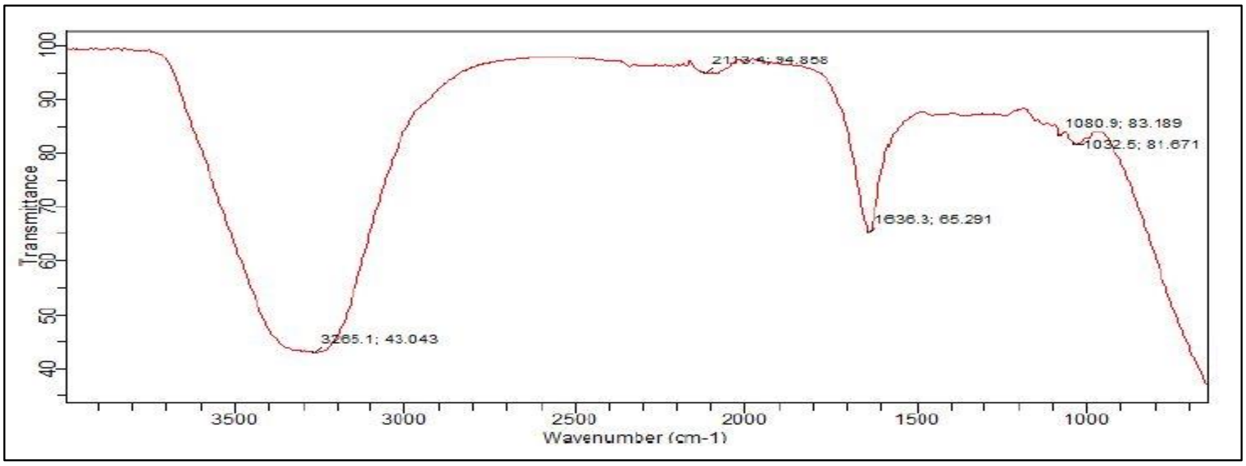

Figure 3: FTIR Image of MgO/ZnO

The Energy Dispersive X-ray (EDX) spectrum of MgO/ZnO nanocomposites (NCs) (Fig. 4) shown above confirms the elemental composition and successful synthesis of the composite material. The prominent peaks for oxygen (O), magnesium (Mg), and zinc (Zn) validate the formation of MgO and ZnO phases within the composite (Murugan *et al.,* 2023). The dominant oxygen peak is indicative of the oxide nature of the nanocomposite, while the relative intensities of Mg and Zn peaks suggest a well-dispersed and stable incorporation of both metal oxides. Such composition is vital in tailoring the physicochemical and functional properties of the material (Uddin *et al.,* 2024). Recent research has highlighted the synergistic effects of combining MgO and ZnO at the nanoscale, resulting in improved photocatalytic, antimicrobial, and electronic properties. According to Ramesh et al. (2024), MgO/ZnO NCs demonstrate enhanced photocatalytic degradation of dyes due to improved electron–hole separation and increased surface area. Similarly, Alfei *et al.,* (2024) reported improved antibacterial performance against E. coli and *S. aureus* due to the combined reactive oxygen species (ROS) generation by both oxides. The presence of Mg enhances the basicity and stability of ZnO, making the composite suitable for environmental and biomedical applications (Shin *et al.,* 2025).

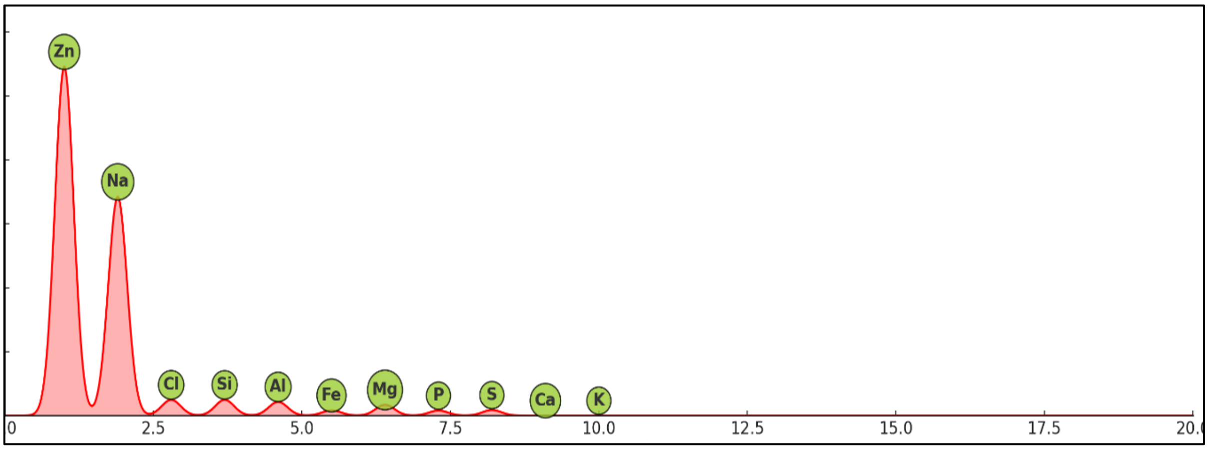

Figure 4: EDS Image of MgO/ZnO

The MgO/ZnO nanocomposite exhibited the highest surface area (282.762 m²/g), pore volume (0.170 cc/g), and slightly reduced pore size (2.800 nm) compared to the individual oxides (Yang *et al.,* 2023). These findings align with recent research by Gado et al. (2025), who reported that binary oxide composites generally possess superior surface characteristics due to their heterogeneous structure, enhancing adsorption efficiency. Similarly, Aalami et al. (2024) observed that MgO/ZnO nanocomposites synthesized via co-precipitation exhibited a higher BET surface area than their monometallic counterparts, improving their capacity in contaminant removal applications. The slight reduction in pore size in the MgO/ZnO could indicate tighter mesoporous structures, beneficial for selective adsorption processes (Tu & Cai, 2024). The improved physicochemical properties of the MgO/ZnO composite suggest its potential for superior performance in adsorption-related environmental applications, confirming findings from other recent nanomaterial-based adsorption studies (Hamad *et al.,* 2024).

Table 1: Summary of BET Results of MgO/ZnO

Adsorbent	Surface Area (m²/g)	Pore size (nm)	Pore volume (cc/g)
MgO/ZnO	282.762	2.800	0.170

The analysis of tannery wastewater in Table 2 reveals that most physicochemical parameters fall within the acceptable limits of WHO/FEPA standards, indicating a generally moderate level of pollution. Parameters such as pH (6.5), temperature (38 °C), TSS (45 mg/L), TDS (950 mg/L), COD (200 mg/L), BOD (45 mg/L), and others comply with permissible limits, suggesting minimal organic and inorganic load. However, heavy metals such as Chromium (Cr: 0.12 mg/L), Lead (Pb: 0.08 mg/L), and Cadmium (Cd: 0.01 mg/L) exceed the recommended limits (0.05 mg/L, 0.01 mg/L, and 0.003 mg/L respectively), posing significant environmental and health concerns (Ma *et al.,* 2020). Recent studies align with these findings. For instance, Arti &Mehra (2023) reported elevated Cr and Pb levels in tannery effluents in Pakistan, citing dermal and systemic toxicity risks. Similarly, Oladimeji *et al.,* (2022) observed high Cd concentrations in wastewater from leather industries in Nigeria, emphasizing its bioaccumulation in aquatic organisms. The moderately low COD and BOD values in this study also reflect partial biodegradability of the wastewater, consistent with findings by Periyasamy, (2024), who highlighted improvements in wastewater quality due to improved pre-treatment practices in some tanneries. Despite progress, the elevated toxic metals underline the need for stricter regulatory enforcement and adoption of advanced treatment technologies (Zhang *et al.,* 2024).

Table 2: Physicochemical Parameters of Tannery Wastewater

Parameters	Tannery Wastewater Value	Standard Limit (WHO/FEPA)
pH	6.5	6.5 - 8.5
Temperature (°C)	38	<40
Total Suspended Solids (TSS) (mg/L)	45	30 - 50
Total Dissolved Solids (TDS) (mg/L)	950	500 - 1000
Chemical Oxygen Demand (COD) (mg/L)	200	250
Biological Oxygen Demand (BOD) (mg/L)	45	50
Electrical Conductivity (µS/cm)	1400	1000 - 1500

Parameters	Tannery Wastewater Value	Standard Limit (WHO/FEPA)
Chloride (Cl^-) (mg/L)	200	250
Sulfide (S^{2-}) (mg/L)	0.04	0.05
Chromium (Cr) (mg/L)	0.12 ↑	0.05
Lead (Pb) (mg/L)	0.08 ↑	0.01
Cadmium (Cd) (mg/L)	0.01 ↑	0.003
Zinc (Zn) (mg/L)	0.4	3.0
Iron (Fe) (mg/L)	2.40↑	1.0
Copper (Cu) (mg/L)	0.2	2.0

The removal efficiency of Pb, Cd, Fe, and Cr ions from tannery wastewater using MgO/ZnO nanocomposite shows a clear dependence on contact time, which is a critical operational parameter in adsorption processes (Fig. 5). At the initial stage (0 minutes), the removal of all metal ions is naturally zero because the adsorbent and solution have not interacted sufficiently. However, after only 10 minutes of contact, there is a significant uptake for all metals, with Pb, Cd, Fe, and Cr removals reaching 25.16%, 27.16%, 31.90%, and 32.06%, respectively. This rapid initial adsorption can be attributed to the large number of vacant active sites available on the MgO/ZnO surface, as well as the high concentration gradient between the metal ions in solution and the adsorbent surface (Ata *et al.,* 2023). The nanocomposite's high surface area and reactive metal oxide functionalities enhance its ability to interact with the positively charged metal ions through electrostatic attraction and surface complexation (Idris *et al.,* 2024). Between 10 and 20 minutes, removal efficiencies continue to rise, although the rate of increase is somewhat slower for some metals. Pb increases from 25.16% to 31.50%, Cd from 27.16% to 33.60%, Fe from 31.90% to 50.25%, and Cr from 32.06% to 40.70%. The sharp increase in Fe removal in this period suggests that Fe ions have a higher affinity for the MgO/ZnO surface, possibly due to their smaller hydrated ionic radius or stronger surface complexation tendencies (Abdelrahman *et al.,* 2024). At this stage, intraparticle diffusion begins to contribute to the adsorption process, as external surface sites start to saturate and ions diffuse into the pores of the nanocomposite (Elkhatib *et al.,* 2022). From 20 to 30 minutes, the removal rates for all metals rise markedly, with Pb reaching 40.52%, Cd 48.90%, Fe 62.12%, and Cr 56.15%. This phase represents a balance between the availability of active sites and the increasing competition between ions for adsorption. The higher increases in Cd, Fe, and Cr removals compared to Pb suggest stronger binding energies or faster diffusion rates for these ions (Ata *et al.,* 2023). Between 30 and 40 minutes, adsorption continues to rise but at a slower rate, indicating that the system is approaching equilibrium. Pb increases to 45.60%, Cd to 52.63%, Fe to 68.10%, and Cr to 62.14%. The slower increment reflects the gradual saturation of available sites and the increasing importance of slower intraparticle diffusion and pore-filling mechanisms (Abdelrahman *et al.,* 2024). At 50 minutes, maximum removal for most metals is achieved: Pb at 55.42%, Cd at 58.10%, Fe at 68.03% (slightly lower than at 40 minutes, indicating possible desorption or competition effects), and Cr at 69.03%. The high Cr removal suggests a strong chemical affinity between Cr species and the MgO/ZnO surface, likely due to specific adsorption or inner-sphere complexation (Elkhatib *et al.,* 2022). At 60 minutes, there is a slight decline in removal efficiency for Pb (52.15%), Cd (56.77%), and Fe (65.03%), while Cr remains relatively stable (67.14%). This decline can be attributed to desorption or ion exchange processes, where weaker-bound ions are displaced by other species in the solution. It may also indicate the onset of saturation equilibrium, where adsorption–desorption dynamics are balanced (Idris *et al.,* 2024). The contact time study reveals that the MgO/ZnO nanocomposite is highly effective in rapidly adsorbing heavy metals from tannery wastewater, with substantial removal occurring within the first 30 minutes. The adsorption process is initially driven by surface interactions and later by pore diffusion, with an optimal contact time of around 50 minutes for maximum removal. Beyond this point, prolonged contact may lead to slight decreases in efficiency due to desorption and competitive effects among metal ions (Ata *et al.,* 2023; Idris *et al.,* 2024). These findings suggest that MgO/ZnO nanocomposite could be a promising adsorbent for treating tannery wastewater, with the advantage of fast adsorption kinetics and strong affinity for multiple heavy metals (Elkhatib *et al.,* 2022).

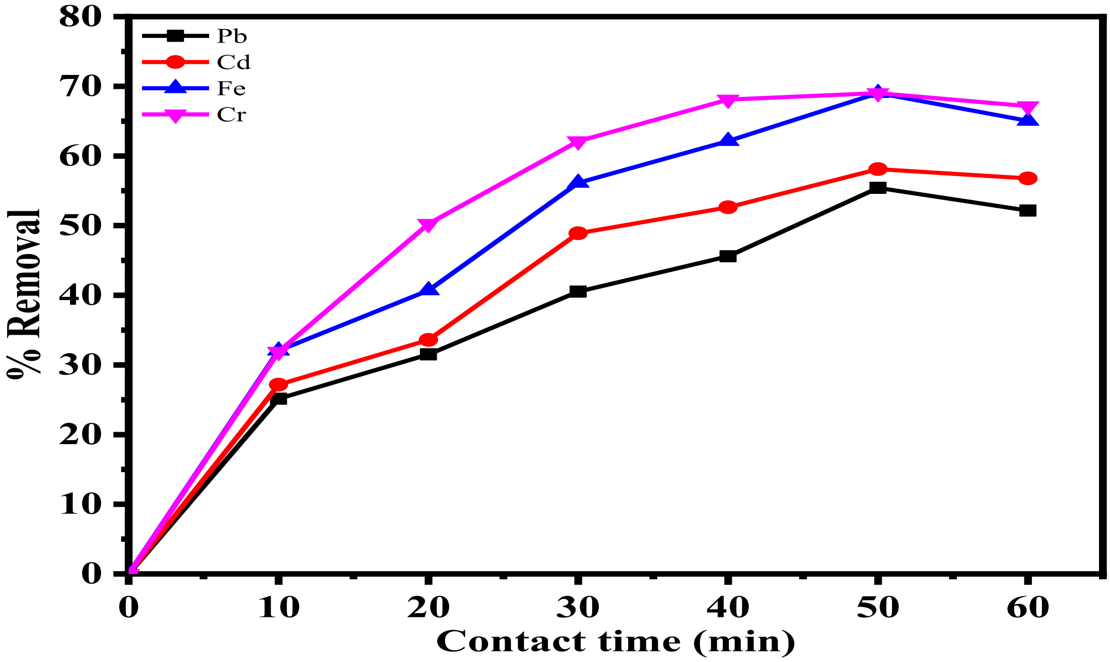

Figure 5: Influence of contact time on the removal of metals using MgO/ZnO

(Fig. 6). In this study, the removal efficiencies for these metals were evaluated at various MgO/ZnO nanocomposite dosages ranging from 0.3 g to 0.8 g. The results show a consistent increase in metal removal as the dosage increases, indicating that MgO/ZnO nanocomposite provide more active sites for adsorption and precipitation processes when present in higher amounts (Leiva *et al.,* 2021; Chauhan *et al.,* 2023). At the lowest dosage tested (0.3 g), the removal efficiency was moderate for Pb (40.07%) and Fe (46.31%), while Cd recorded the highest removal (94.52%) and Cr achieved 52.10%. This suggests that at low nanoparticle concentrations, MgO/ZnO nanocomposite has a particularly strong affinity for Cd, possibly due to its smaller ionic radius and higher mobility in solution, allowing it to bind more effectively to the active surfaces of the nanoparticles (Leiva *et al.,* 2021). On the other hand, Pb removal is comparatively lower, likely due to competition with other cations or slower diffusion rates (Saod *et al.,* 2023). Increasing the dosage to 0.4 g resulted in substantial improvements for Pb (56.41%), Fe (70.25%), and Cr (72.14%), though Cd removal surprisingly decreased to 66.81%. This drop for Cd might be due to partial re-dissolution of adsorbed Cd ions under certain pH conditions or competition from other metal ions that increasingly occupy active sites as MgO/ZnO dosage increases (Praipipat *et al.,* 2024). Nevertheless, Fe and Cr removal improved considerably at this stage, highlighting the enhanced surface area and increased number of reactive sites available for these ions. At 0.5 g dosage, there was a significant jump in the removal efficiency of all metals, with Pb at 69.80%, Cd at 72.40%, Fe at 88.81%, and Cr at 88.42%. This shows that the availability of MgO/ZnO nanocomposite in greater amounts promotes better adsorption kinetics, reduces competition for active sites, and allows for more complete precipitation or complexation reactions between the metal ions and MgO/ZnO (Chauhan *et al.,* 2023; Leiva *et al.,* 2021). When the dosage reached 0.6 g, Pb removal improved dramatically to 84.06%, Cd to 83.36%, Fe to 90.08%, and Cr to 92.57%. This stage represents a near-optimal balance where the surface area of MgO/ZnO nanocomposite is sufficient to interact with almost all available metal ions in the wastewater. The sharp increase for Pb indicates that higher dosages help overcome the initial kinetic limitations seen at lower concentrations, allowing for stronger and faster binding (Leiva *et al.,* 2021; Saod *et al.,* 2023). At 0.7 g, the removal efficiencies were extremely high: Pb (92.10%), Cd (94.01%), Fe (96.10%), and Cr (96.78%). This performance suggests that MgO/ZnO nanocomposite at this dosage can remove nearly all the targeted metal ions, likely due to saturation of binding and reactive sites with metals and enhanced precipitation of metal hydroxides in the presence of MgO/ZnO (Chauhan *et al.,* 2023; Zaidi *et al.,* 2025). At the maximum dosage of 0.8 g, the removal efficiencies reached their peak: Pb (96.07%), Cd (97.70%), Fe (98.10%), and Cr (99.01%). At this level, the availability of active sites far exceeds the concentration of metal ions in the wastewater, ensuring almost complete removal. The high performance across all metals suggests that MgO/ZnO nanocomposite are exceptionally effective adsorbents and co-precipitation agents for treating tannery wastewater when used at sufficient dosages (Leiva *et al.,* 2021; Samejo *et al.,* 2025).

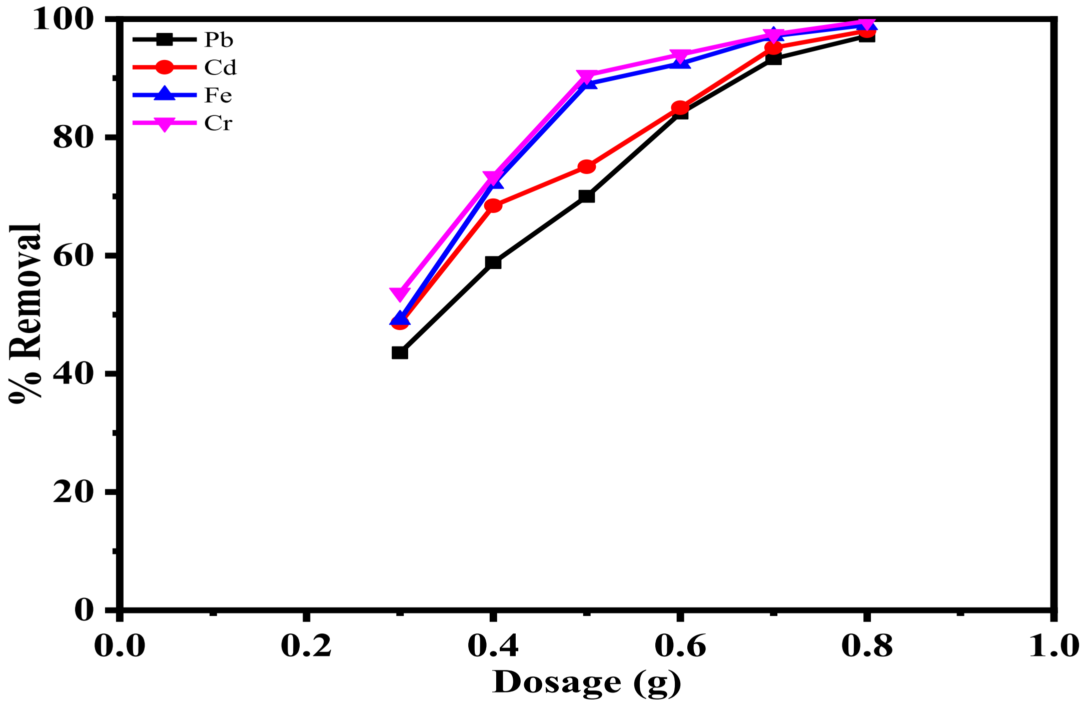

Figure 6: Influence of dosage on the removal of metals using MgO/ZnO

The effect of dosage on the removal of lead (Pb), cadmium (Cd), iron (Fe), and chromium (Cr) from tannery wastewater using ZnO/MgO shows a clear trend of increasing removal efficiency with increasing dosage (Fig. 6). At the lowest dosage of 0.3 g, the removal percentages were relatively moderate, with Pb (43.55%), Cd (48.6%), Fe (49.15%), and Cr (53.67%). This indicates that at low adsorbent dosage, the number of available active sites is limited, resulting in reduced removal efficiency. When the dosage was increased to 0.4 g, there was a notable improvement in metal removal, with Pb rising to 58.8%, Cd to 68.41%, Fe to 72.16%, and Cr to 73.4%. This shows that the increase in adsorbent dosage enhances the availability of surface area and binding sites for metal ion uptake, thereby improving efficiency. At 0.5 g dosage, the removal efficiency continued to rise significantly, with Pb at 70.01%, Cd at 75.01%, Fe at 89.01%, and Cr at 90.52%. The sharp improvement in Fe and Cr removal at this stage suggests a strong affinity of the adsorbent towards these metals. Further increase to 0.6 g dosage resulted in higher removal, where Pb reached 84.1%, Cd 85.01%, Fe 92.46%, and Cr 94.01%. This steady increment indicates that more metal ions were captured due to the greater availability of adsorption sites. At 0.7 g dosage, the removal became very high for all metals: Pb (93.3%), Cd (95.16%), Fe (97.13%), and Cr (97.42%). This shows that near-optimal adsorption capacity was being approached, as the majority of the metal ions were already removed. At the maximum dosage of 0.8 g, the highest efficiencies were recorded: Pb (97.15%), Cd (98.03%), Fe (99.01%), and Cr (99.66%). At this level, almost complete removal of the metals was achieved, demonstrating that dosage plays a critical role in maximizing adsorption efficiency. The trend clearly shows that increasing the adsorbent dosage significantly enhances metal removal due to the increased number of available active sites and surface area for binding. However, at higher dosages (0.7–0.8 g), the removal efficiencies approach saturation, indicating that further increases may not result in substantial improvements since most of the metal ions are already removed from the solution. This observation aligns with earlier reports on nanomaterial-based adsorbents, where increased dosage generally leads to greater pollutant removal until equilibrium or saturation is achieved (Singh *et al.,* 2021). Similar findings were noted in the use of magnesium oxide nanoparticles incorporated into rice husk ash, where dosage significantly influenced the adsorption of Pb(II) and Cr(VI) ions (Mustapha *et al.,* 2024). Likewise, MgO/activated carbon nanocomposites have shown dosage-dependent efficiency in treating organic and inorganic pollutants from abattoir wastewater (Idris *et al.,* 2024). Furthermore, binary nanocomposites such as MgO/CuO and MgO/Cu_3MgO_4 have demonstrated that higher dosages enhance metal ion disposal performance, particularly for Zn(II) ions (Abdelrahman *et al.,* 2024).

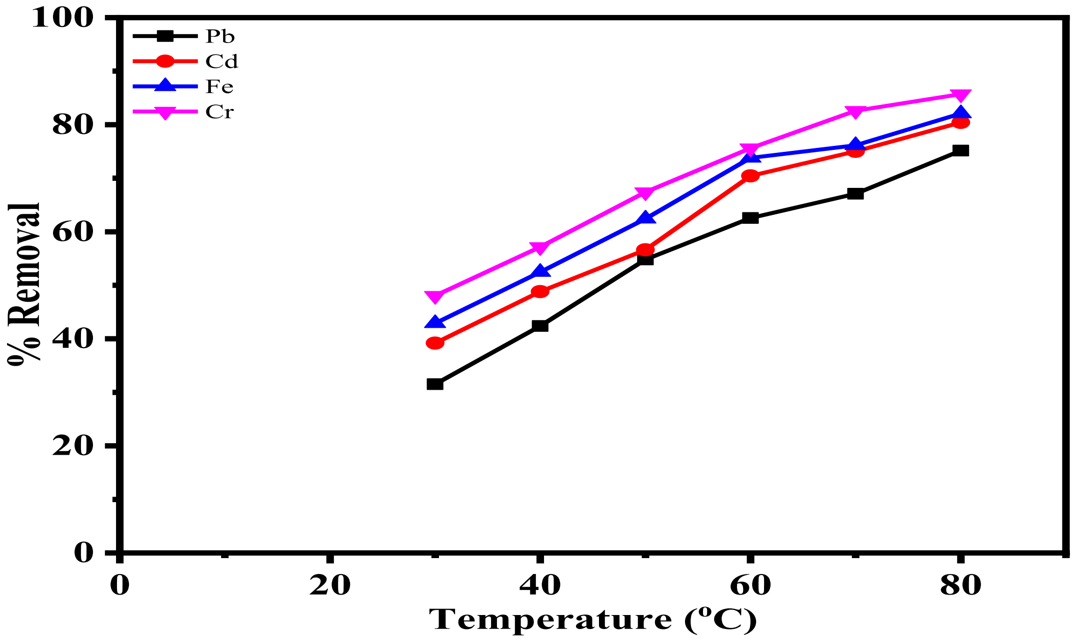

Figure 7: Influence of temperature on the removal of metals using MgO/ZnO

The MgO/ZnO composite records the highest KF values overall, ranging from 2.921 (Pb) to 3.651 (Cr). This result highlights the synergistic effect of combining MgO and ZnO, producing a composite with more efficient surface properties (Idris *et al.,* 2024). The n values (1.871–1.970) remain favorable, reflecting abundant adsorption sites, while the consistently higher R^2 values indicate that the Freundlich model describes the composite better than the individual oxides. From the Freundlich isotherm, adsorption is favorable across all metals and adsorbents, with chromium showing the highest adsorption intensity. However, because its R^2 values are generally lower than those of other models, Freundlich is not the best-fitting model overall. The MgO/ZnO composite once again demonstrates the best performance, with qmax values of 96.12 mg/g (Pb), 105.81 mg/g (Cd), 112.05 mg/g (Fe), and 119.81 mg/g (Cr). Its K_L values are also consistently higher, reflecting enhanced affinity for the metals (Idris *et al.,* 2024). With very high R^2 values (0.9920–0.9991), the Langmuir model describes the composite's adsorption behavior with great accuracy. Overall, the Langmuir model fits the experimental data better than the Freundlich model, confirming that adsorption occurs mainly through monolayer coverage of active sites (Singh *et al.,* 2021). The MgO/ZnO composite records the highest Qmax values overall (125.18–180.21 mg/g), surpassing the individual oxides. Its adsorption energies range from 20.97 kJ/mol (Pb) to 31.44 kJ/mol (Cr), once again confirming strong chemisorption (Idris *et al.,* 2024). With nearly perfect R^2 values (0.9934–0.9996), the D–R model provides an excellent fit. The D–R model confirms that adsorption is chemical in nature for all tested metals and adsorbents. The energy values indicate stronger binding for Cr, followed by Fe, Cd, and Pb. This agrees with the observed adsorption trend and demonstrates that chemisorption dominates the removal process (Singh *et al.,* 2022).

Table 3: Isotherm Parameters for the removal of some metal ions from tannery wastewater

Adsorbent	Metal	Freundlich			Langmuir			D-R			
		K_F	n	R^2	K_L	q_{max}	R^2	Q_{max}	b	E	R^2
MgO/ZnO	Pb	2.921	1.871	0.9316	0.0911	96.12	0.9920	125.18	20.97	4×10^{-4}	0.9934
	Cd	3.186	1.890	0.9408	0.123	105.81	0.9970	152.51	24.24	4×10^{-5}	0.9981
	Fe	3.470	1.961	0.9631	0.135	112.05	0.9986	172.30	27.08	4×10^{-5}	0.9992
	Cr	3.651	1.970	0.9770	0.141	119.81	0.9991	180.21	31.44	4×10^{-6}	0.9996

The highest k_1 value is recorded for chromium with the MgO/ZnO composite (0.121 min^{-1}), suggesting that Cr has the fastest initial uptake compared to the other metals. This observation indicates that chromium interacts strongly with the adsorbent surfaces at the beginning of the process, consistent with its well-known tendency to form strong interactions with metal oxides (Chauhan *et al.,* 2023). The equilibrium adsorption capacities (q_e) predicted by this model range from 42.40 to 91.61 mg/g, with the maximum observed for Cr on the MgO/ZnO composite. However, the pseudo-first-order model generally underestimates q_e compared to experimental values derived from the pseudo-second-order model, showing that it does not fully capture the actual adsorption mechanism (Elkhatib *et al.,* 2022). The correlation coefficients (R^2) for this model lie between 0.8240 and 0.9408, which are lower than those obtained for the pseudo-second-order model. Although Cr adsorption gives relatively higher R^2 values (0.9181–0.9408), suggesting that first-order kinetics plays some role in the initial stage, the overall fit remains weaker than the second-order description. According to the data, the pseudo-second-order rate constants (k_2) range from 1.867 to 7.215 g/mg·min, with the highest value observed for Cr on MgO/ZnO (7.215). This confirms the strong and rapid interaction of chromium with the composite surface (Chauhan *et al.,* 2023). The equilibrium adsorption capacities (q_e) predicted by this model are much higher than those from the pseudo-first-order model, ranging from 68.21 mg/g for Pb on MgO to 116.41 mg/g for Cr on MgO/ZnO. These values align closely with the experimental results, making the pseudo-second-order model the most reliable description of the adsorption process (Ata *et al.,* 2023; Elkhatib *et al.,* 2022). The correlation coefficients (R^2) for this model are very high, ranging from 0.9625 to 0.9930, showing an excellent fit to the data. Once again, Cr on MgO/ZnO records the highest α value (0.821), reflecting its rapid and efficient uptake by the composite. Chromium adsorption on MgO/ZnO shows the highest β (0.0830), confirming that strong chemisorption dominates the process (Chauhan *et al.,* 2023). The correlation coefficients (R^2) for the Elovich model range from 0.8831 to 0.9556, which are moderately high. Although not as strong as the pseudo-second-order fits, these values still indicate a reasonable level of agreement, particularly for Cr (0.9556) and Fe (0.9407). This suggests that surface heterogeneity plays an important role in the adsorption of these metals, especially when using the MgO/ZnO composite (Samejo *et al.,* 2025).

Table 4: Kinetic Parameters for the removal of some metal ions from tannery wastewater

Adsorbent	Metal	Pseudo-first			Pseudo-second			Elovich		
		k_1	q_e	R^2	k_2	q_e	R^2	a	b	R^2
MgO/ZnO	Pb	0.0618	59.62	0.8860	2.430	95.65	0.9871	0.201	0.0408	0.9178
	Cd	0.0820	70.81	0.9117	3.715	103.46	0.9902	0.462	0.0512	0.9316
	Fe	0.0916	83.30	0.9340	5.807	111.19	0.9916	0.690	0.0691	0.9407
	Cr	0.121	91.61	0.9408	7.215	116.41	0.9924	0.821	0.0830	0.9556

The three key thermodynamic variables considered include the standard enthalpy change (ΔH), the standard entropy change (ΔS), and the Gibbs free energy change (ΔG) at various temperatures ranging from 303 to 353 K. The enthalpy values for all the metal–adsorbent systems are positive, ranging from 45.25 to 57.84 kJ/mol. This indicates that the adsorption of Pb, Cd, Fe, and Cr onto MgO/ZnO is endothermic in nature, which agrees with earlier findings that reported positive ΔH values for heavy metal adsorption on oxide-based and clay-derived adsorbents (Chakrabarty *et al.,* 2024). Endothermic adsorption suggests that higher temperatures favor the adsorption process, as energy is required for the interaction between the metal ions and the surface functional groups of the adsorbents. Among the adsorbents, the binary composite (MgO/ZnO) recorded the highest enthalpy changes, especially for Cr removal (57.84 kJ/mol). This suggests that the hybrid material possesses stronger affinity and binding interactions with the metal ions compared to the individual oxides, consistent with the enhanced performance of other oxide-based nanocomposites in heavy metal removal (Fouda-Mbanga *et al.,* 2024). The entropy values (ΔS) are positive for all adsorption systems, ranging from 22.67 to 37.01 kJ/mol·K. A positive entropy change signifies an increase in randomness at the solid–solution interface during adsorption. This increase in disorder may be attributed to the release of water molecules or counter-ions from the hydration shells of the metal ions when they are adsorbed onto the solid surface (Malima *et al.,* 2021). Among the adsorbents, MgO/ZnO exhibited the highest entropy values, particularly for Fe and Cr, which further supports its superior performance.

Table 5: Thermodynamic Parameters for the removal of some metal ions from tannery wastewater

Adsorbent	Metal	ΔH (kJ/mol)	ΔS (kJ/mol.K)	ΔG (kJ/mol)					
				303	313	323	333	343	353
MgO/ZnO	Pb	49.04	28.73	-8.66	-8.94	-9.23	-9.52	-9.81	-10.09
	Cd	51.5	29.02	-8.74	-9.03	-9.32	-9.61	-9.90	-10.19
	Fe	54.66	36.02	-10.86	-11.22	-11.58	-11.94	-12.30	-12.66
	Cr	57.84	37.01	-11.16	-11.53	-11.90	-12.27	-12.64	-13.01

CONCLUSION

The production of MgO/ZnO nanocomposite is a promising, efficient, and sustainable option in the removal of toxic metals in tannery wastewater. The synthesized nanocomposite had high surface area, adsorption capacity and synergistic performance owing to cumulative characteristics of ZnO and MgO. Its high capacity of reducing concentrations of chromium, cadmium, lead, and nickel by a large percentage implies that it can be used on an industrial level. In addition, it is cost and environmentally-friendly and can be integrated into the current treatment systems. The research will help in the development of nanotechnology-based wastewater treatment and in the adoption of cleaner production and environmental conservation in the leather manufacturing industry.

REFERENCES

- Aalami, Z., Hoseinzadeh, M., Hosseini Manesh, P., Aalami, A. H., Es'haghi, Z., Darroudi, M., Sahebkar, A., & Hosseini, H. A. (2024). Synthesis, characterization, and photocatalytic activities of green sol-gel ZnO nanoparticles using Abelmoschus esculentus and Salvia officinalis: A comparative study versus co-precipitation-synthesized nanoparticles. Heliyon, 10(2), e24212. https://doi.org/10.1016/j.heliyon.2024.e24212
- Abdelrahman, E.A., Khalil, M.M., Algethami, F.K., Khairy, M., Abou El-Reash, Y.G., Saad, F.A., Shah, R.K. and Ammar, A.M., 2024. Facile synthesis of MgO/CuO and MgO/Cu3MgO4 binary nanocomposites as promising adsorbents for the disposal of Zn (II) ions. *Journal of Inorganic and Organometallic Polymers and Materials*, *34*(1), pp.266-281.
- Alfei, S., Schito, G. C., Schito, A. M., & Zuccari, G. (2024). Reactive Oxygen Species (ROS)-Mediated Antibacterial Oxidative Therapies: Available Methods to Generate ROS and a Novel Option Proposal. International journal of molecular sciences, 25(13), 7182. https://doi.org/10.3390/ijms25137182
- Alharbi, F. N., Abaker, Z. M., & Makawi, S. Z. A. (2023). Phytochemical Substances—Mediated Synthesis of Zinc Oxide Nanoparticles (ZnO NPS). Inorganics, 11(8), 328. https://doi.org/10.3390/inorganics11080328
- Almoneef, M. M., Awad, M. A., Aldosari, H. H., Hendi, A. A., Aldehish, H. A., Merghani, N. M., & Alshammari, S. G. (2024). Exploring the multi-faceted potential: Synthesized ZnO nanostructure - Characterization, photocatalysis, and crucial biomedical applications. Heliyon, 10(12), e32714. https://doi.org/10.1016/j.heliyon.2024.e32714
- Ameen, F. (2023). Improving Tannery Wastewater Treatments Using an Additional Microbial Treatment with a Bacterial–Fungal Consortium. *Biology*, *12*(12), 1507. https://doi.org/10.3390/biology12121507
- Arti, L. & Mehra, R. (2023). Analysis of heavy metals and toxicity level in the tannery effluent and the environs. Environmental monitoring and assessment, 195(5), 554. https://doi.org/10.1007/s10661-023-11154-4
- Ata, S., Tabassum, A., Shaheed, I., ul Mohsin, I., Alwadai, N., Al Huwayz, M., Iqbal, M. and Nazir, A., 2023. Adsorption Thermodynamics, Modeling, and Kinetics Studies for the Removal of Lead Ions Using ZnO Nanorods. *Adsorption Science & Technology*, *2023*, p.7740674.
- Chakrabarty, S., Mim, R. M., Tonu, N. T., Ara, M. H., & Dhar, P. K. (2024). Removal of Toxic Pb (II) Ion from Aqueous Solution Using ZnO/K2SO4 Nanocomposites: Kinetics, Isotherms and Error Function Analyses. *Chemistry Africa*, *7*(3), 1467-1480.
- Chauhan, A. K., Kataria, N., Gupta, R., & Garg, V. K. (2023). Biogenic fabrication of ZnO@ EC and MgO@ EC using Eucalyptus leaf extract for the removal of hexavalent chromium Cr (VI) ions from water. *Environmental Science and Pollution Research*, *30*(60), 124884-124901.
- Cortés, E., Wendisch, F. J., Sortino, L., Mancini, A., Ezendam, S., Saris, S., de S Menezes, L., Tittl, A., Ren, H., & Maier, S. A. (2022). Optical Metasurfaces for Energy Conversion. Chemical reviews, 122(19), 15082–15176. https://doi.org/10.1021/acs.chemrev.2c00078
- Elkhatib, E. A., Moharem, M. L., Saad, A. F., & Attia, F. A. (2022). Novel metal-based nanocomposite for rapid and efficient removal of lead from contaminated wastewater sorption kinetics, thermodynamics and mechanisms. *Scientific Reports*, *12*(1), 8412.
- Fouda-Mbanga, B. G., Pillay, K., & Tywabi-Ngeva, Z. (2024). Novel development of zinc oxide–coated carbon nanoparticles from pineapple leaves using sol gel method for optimal adsorption of Cu2+ and reuse in latent fingerprint application. *Environmental Science and Pollution Research*, *31*(27), 38801-38820.
- Gado, W. S., Morshedy, A. S., Masoud, A. M., Mohammed, A. E. M. E., Taha, E. H., El-Zahhar, A. A., Alghamdi, M. M., Naggar, A. M. A. E., & El-Fawal, E. M. (2025). Ultrasound-assisted synthesis of biomass-derived carbon-supported binary metal oxides for efficient adsorption of heavy metals from wastewater. RSC advances, 15(17), 13662–13680. https://doi.org/10.1039/d5ra00057b
- Hamad, M. T. M. H., & Ibrahim, S. (2024). Effective fabrication and characterization of eco-friendly nano particles composite for adsorption Cd (II) and Cu (II) ions from aqueous solutions using modelling studies. Scientific reports, 14(1), 11767. https://doi.org/10.1038/s41598-024-61050-1
- Ibrahim, S. Z., Muhammad, A., Saidu, B., Tsado, A. N. Mathew, J. T**.,** Kolo, O. O., Zubairu, R., Joseph, D., Suleman, B. A., Danazumi, N., Dabogi, J. Y. & Mustapha, S. (2025). Utilization of Zeolite-A/ZnO/Graphene Oxide Nanocomposite in the Adsorption Removal of some Heavy Metals from Pharmaceutical Wastewater. Sch Int J Chem Mater Sci, 8(3): 117-131.
- Idris A. Y., Elele U. U. and Mathew, J. T. (2024). Preparation and characterization of MoO_3 nanoparticles for the photocatalytic degradation of dyeing wastewater. *Science World Journal Vol.* 19(4), 1006-1011. https://dx.doi.org/10.4314/swj.v19i4.14
- Idris, Y. J., Tijani, J. O., Mustapha, S., Ndamitso, M. M., Abdulkareem, A. S., Egbosiuba, T. C., & Sagadevan, S. (2024). Effective removal of organic and inorganic pollutants from abattoir wastewater using magnesium oxide/activated carbon

nanocomposites. *Ceramics International*, *50*(14), 25933-25947.

- Kiran, B. R., Kopperi, H., & Venkata Mohan, S. (2022). Micro/nano-plastics occurrence, identification, risk analysis and mitigation: challenges and perspectives. Re/views in environmental science and bio/technology, 21(1), 169–203. https://doi.org/10.1007/s11157-021-09609-6
- Lallo da Silva, B., Abuçafy, M. P., Berbel Manaia, E., Oshiro Junior, J. A., Chiari-Andréo, B. G., Pietro, R. C. R., & Chiavacci, L. A. (2019). Relationship Between Structure and Antimicrobial Activity of Zinc Oxide Nanoparticles: An Overview. International journal of nanomedicine, 14, 9395–9410. https://doi.org/10.2147/IJN.S216204
- Leiva, E., Tapia, C., & Rodríguez, C. (2021). Highly efficient removal of Cu (II) ions from acidic aqueous solution using ZnO nanoparticles as nano-adsorbents. *Water*, *13*(21), 2960.
- Ma, J., Wu, S., Shekhar, N. V. R., Biswas, S., & Sahu, A. K. (2020). Determination of Physicochemical Parameters and Levels of Heavy Metals in Food Waste Water with Environmental Effects. Bioinorganic chemistry and applications, 2020, 8886093. https://doi.org/10.1155/2020/8886093
- Malima, N. M., Owonubi, S. J., Lugwisha, E. H., & Mwakaboko, A. S. (2021). Thermodynamic, isothermal and kinetic studies of heavy metals adsorption by chemically modified Tanzanian Malangali kaolin clay. *International Journal of Environmental Science and Technology*, *18*(10), 3153-3168.
- Mathew, J. T., Inobeme, A., Shaba, E. Y., Musah, M., Azeh, Y., Abubakar, H., Adam, I. B., Muhammad, A. I., Muhammad, H. A., Ismail, H., Umar, M. T., Aliyu, M. S., Yisa, S. P., Ismaila, A. O., Etsuyankpa, M. B., Musa, S. T., Mamman, A. (2025). Adsorptive Removal of Cu^{2+}, Pb^{2+}, and Cr^{6+} from Pharmaceutical Wastewater Using Graphene/Rutile (TiO_2) Nanocomposites. Science World Journal, 20 (3), 1263-1272. https://dx.doi.org/10.4314/swj.v20i3.50
- Mathew, J. T**.**, Inobeme, A., Musah, M., Azeh, Y., Abdullahi, A., Shaba E. Y., Salihu, A. M., Muhammad, E. B., Josiah, J. G., Jibrin, N. A., Ismail, H., Muhammad, A. I., Maurice, J., Mamman, A. & Ndamitso, M. M. (2024) a. A Critical Review of Green Approach on Wastewater Treatment Strategies. *Journal of Applied Science and Environmental Management,* 28(2), 363-391. doi: https://dx.doi.org/10.4314/jasem.v28i2.9
- Mathew, J. T., Musah, M., Azeh, Y. & Muhammed, M. (2024) b. Development of Fe_3O_4 Nanoparticles for the Removal of Some Toxic Metals from Pharmaceutical Wastewater. Caliphate Journal of Science & Technology (CaJoST), 6(1), 26-34. Doi: https://dx.doi.org/10.4314/cajost.v6i1.4
- Mathew, J. T., Musah, M., Azeh, Y. and Musa, M. (2024) c. Removal of Some Toxic Metals from Pharmaceutical Wastewater Using Geopolymer/Fe_3O4/ZnO nanocomposite: Isotherm, Kinetics and Thermodynamic Studies. Confluence University Journal of Science and Technology, 1(1): 50-58. Doi: 10.5455/CUJOSTECH.240706.
- Mathew, J. T., Musah, M., Azeh, Y. & Muhammed, M. (2023) a. Adsorptive Removal of Selected Toxic Metals from Pharmaceutical Wastewater using Fe_3O_4/ZnO Nanocomposite, *Dutse Journal of Pure and Applied Sciences*, 9(4a), 236- 248. https://dx.doi.org/10.4314/dujopas.v9i4a.22.
- Mathew, J. T., Musah, M., Azeh, Y. & Muhammed, M. (2023) b. Kinetic Study of Heavy Metals Removal from Pharmaceutical Wastewater Using Geopolymer/Fe_3O_4 Nanocomposite. Bima Journal of Science and Technology, 7(4), 152- 163. Doi: 10.56892/bima. v7i4.539.
- Milanković, V., Tasić, T., Leskovac, A., Petrović, S., Mitić, M., Lazarević-Pašti, T., Novković, M., & Potkonjak, N. (2024). Metals on the Menu—Analyzing the Presence, Importance, and Consequences. *Foods*, *13*(12), 1890. https://doi.org/10.3390/foods13121890
- Mtavangu, S. G., Machunda, R. L., van der Bruggen, B., & Njau, K. N. (2022). In situ facile green synthesis of Ag-ZnO nanocomposites using Tetradenia riperia leaf extract and its antimicrobial efficacy on water disinfection. Scientific reports, 12(1), 15359. https://doi.org/10.1038/s41598-022-19403-1
- Muhammad, M. S., Musah, M. and Mathew, J. T. (2024). Preparation and Characterization of Activated Carbon from Africa Star Apple (Chrysophyllum albidum) Seed Shell. FUDMA Journal of Sciences (FJS), 8(3), 194-199. DOI: https://doi.org/10.33003/fjs-2024-0803-2485
- Murugan, S., Ashokkumar, M., Sakthivel, P., & Choi, D. (2023). Sulfur deficiency mediated visible emission of ZnS QDs by magnesium dopant and their application in waste water treatment. Heliyon, 9(7), e17947. https://doi.org/10.1016/j.heliyon.2023.e17947
- Musah M., Mathew J.T., Azeh Y (2025). Synthesis, Characterization and Application of ZnO/GO/Zeolite-A Nanocomposite in the Sorption of Selected Heavy Metals from Pharmaceutical Effluent. Sch Int J Chem Mater Sci, 8(5): 202-212.
- Musa A. V., Musah, M. and Mathew, J. T. (2024). Production and characterization of Zeolite-A nanoparticles for the treatment of pharmaceutical wastewater. *Science World Journal Vol.* 19(4), 987-993. https://dx.doi.org/10.4314/swj.v19i4.11
- Mustapha, L. S., Jacob-Oricha, S. O., Yahya, M. D., Lau, S. Y., Yusuff, A. S., & Obayomi, K. S. (2024). Effective removal of Cr (VI) and Pb (II) ions from mining wastewater using eco-friendly synthesized

magnesium oxide nanoparticles incorporated rice husk ash. *Environmental Advances*, *15*, 100507.

- Oladimeji, T. E., Oyedemi, M., Emetere, M. E., Agboola, O., Adeoye, J. B., & Odunlami, O. A. (2024). Review on the impact of heavy metals from industrial wastewater effluent and removal technologies. Heliyon, 10(23), e40370. https://doi.org/10.1016/j.heliyon.2024.e40370
- Periyasamy, A. P. (2024). Recent Advances in the Remediation of Textile-Dye-Containing Wastewater: Prioritizing Human Health and Sustainable Wastewater Treatment. Sustainability, 16(2), 495. https://doi.org/10.3390/su16020495
- Praipipat, P., Ngamsurach, P., Chatraksa, W., & Charoenphong, V. (2024). Removal of cadmium (II) ions by beaded materials of mangosteen (Garcinia mangostana Linn) modified with magnesium oxide (MgO) and titanium dioxide (TiO2). *Arabian Journal for Science and Engineering*, 1-18.
- Quintard, B., Yang, X., & Wang, L. (2025). Quantitative Modeling of High-Energy Electron Scattering in Thick Samples Using Monte Carlo Techniques. Applied Sciences, 15(2), 565. https://doi.org/10.3390/app15020565
- Ramesh, N., Lai, C. W., Johan, M. R. B., Mousavi, S. M., Badruddin, I. A., Kumar, A., Sharma, G., & Gapsari, F. (2024). Progress in photocatalytic degradation of industrial organic dye by utilising the silver doped titanium dioxide nanocomposite. Heliyon, 10(24), e40998. https://doi.org/10.1016/j.heliyon.2024.e40998
- Redjili, S., Ghodbane, H., Tahraoui, H., Abdelouahed, L., Chebli, D., Ola, M. S., Assadi, A. A., Kebir, M., Zhang, J., Amrane, A., & Lekmine, S. (2025). Green Innovation: Multifunctional Zinc Oxide Nanoparticles Synthesized Using Quercus robur for Photocatalytic Performance, Environmental, and Antimicrobial Applications. Catalysts, 15(3), 256. https://doi.org/10.3390/catal15030256
- Rezania, S., Darajeh, N., Rupani, P. F., Mojiri, A., Kamyab, H., & Taghavijeloudar, M. (2024). Recent Advances in the Adsorption of Different Pollutants from Wastewater Using Carbon-Based and Metal-Oxide Nanoparticles. *Applied Sciences*, *14*(24), 11492. https://doi.org/10.3390/app142411492
- Samejo, S., Baig, J. A., Algethami, F. K., Kazi, T. G., & Akhtar, K. (2025). Green synthesized magnesium oxide nanohybrid as an effective adsorbent for removing toxic metals from contaminated water. *International Journal of Environmental Science and Technology*, 1-14.
- Saod, W. M., Oliver, I. W., Thompson, D. F., Holborn, S., Contini, A., & Zholobenko, V. (2023). Magnesium oxide loaded mesoporous silica: Synthesis, characterisation and use in removing lead and cadmium from water supplies. *Environmental Nanotechnology, Monitoring & Management*, *20*, 100817.
- Sazid, M. G., & Supto, S. T. J. (2025). Advances in Implementation of Metal Oxide Nanoparticles for Urban Water Pollution Treatment. *Engineering Proceedings*, *87*(1), 96. https://doi.org/10.3390/engproc2025087096
- Shin, J., Choi, J., Choi, Y. W., Kim, S., & Hwang, I. (2025). Development and Characterization of Zn-ZnO Nanocomposites for Enhanced Biodegradable Material Properties. Materials, 18(5), 938. https://doi.org/10.3390/ma18050938
- Singh, S., Anil, A.G., Khasnabis, S., Kumar, V., Nath, B., Adiga, V., Naik, T.S.K., Subramanian, S., Kumar, V., Singh, J. and Ramamurthy, P.C., (2022). Sustainable removal of Cr (VI) using graphene oxide-zinc oxide nanohybrid: Adsorption kinetics, isotherms and thermodynamics. *Environmental Research*, *203*, p.111891.
- Singh, S., Kapoor, D., Khasnabis, S., Singh, J., & Ramamurthy, P. C. (2021). Mechanism and kinetics of adsorption and removal of heavy metals from wastewater using nanomaterials. *Environmental Chemistry Letters*, *19*(3), 2351-2381.
- Tu, W., & Cai, W. (2024). Selective Adsorption of Hazardous Substances from Wastewater by Hierarchical Oxide Composites: A Review. Toxics, 12(7), 447. https://doi.org/10.3390/toxics12070447
- Uddin, M. J., Yeasmin, M. S., Muzahid, A. A., Rahman, M. M., Rana, G. M. M., Chowdhury, T. A., Al-Amin, M., Wakib, M. K., & Begum, S. H. (2024). Morphostructural studies of pure and mixed metal oxide nanoparticles of Cu with Ni and Zn. Heliyon, 10(9), e30544. https://doi.org/10.1016/j.heliyon.2024.e30544
- Yang, B., Cui, H., Gao, J., Cao, J., Klobučar, G., & Li, M. (2023). Using a Battery of Bioassays to Assess the Toxicity of Wastewater Treatment Plant Effluents in Industrial Parks. *Toxics*, *11*(8), 702.
- Zaidi, R., Khan, S. U., Farooqi, I. H., Ahmed, F., Alsulami, A., Azam, A., & Allehabi, S. O. (2025). Performance, isotherm, kinetics and mechanism of simultaneous removal of Cr (VI), Cu (II) and F ions by CeO2–MgO binary oxide nanomaterials. *Scientific Reports*, *15*(1), 1431.
- Zhang, Y., Li, Z., Tong, X., Xie, Z., Huang, S., Zhang, Y. E., Ke, H. B., Wang, W. H., & Zhou, J. (2024). Three-dimensional atomic insights into the metal-oxide interface in Zr-ZrO2 nanoparticles. Nature communications, 15(1), 7624. https://doi.org/10.1038/s41467-024-52026-w